IEEE Access
Multidisciplinary | Rapid Review | Open Access Journal

SPECIAL SECTION ON ADVANCED COMMUNICATIONS AND NETWORKING TECHNIQUES FOR WIRELESS CONNECTED INTELLIGENT ROBOT SWARMS

Received March 11, 2020, accepted March 21, 2020, date of publication March 24, 2020, date of current version April 16, 2020.

Digital Object Identifier 10.1109/ACCESS.2020.2983083

Gaussian Parameterized Information Aided Distributed Cooperative Underwater Positioning Algorithm

LINGLING ZHANG[1], (Member, IEEE), CHENGKAI TANG[2], (Member, IEEE), PEILIN CHEN[3], AND YI ZHANG[2]

[1]School of Marine Science and Technology, Northwestern Polytechnical University, Xi'an 710072, China
[2]School of Information and Electronic, Northwest Polytechnic University, Xi'an 710072, China
[3]The 54th Research Institute of China Electronics Technology Group Corporation, Shijiazhuang 050081, China

Corresponding authors: Lingling Zhang (llzhang@nwpu.edu.cn) and Chengkai Tang (cktang@nwpu.edu.cn)

This work was supported in part by the National Natural Science Foundation of China under Grant 61801394 and Grant 61803310, in part by the Fundamental Research Funds for the Central Universities under Grant 3102019HHZY030013 and Grant G2019KY05206, and in part by the Natural Science Basic Research Plan in Shaanxi Province of China under Grant 2020JQ-202.

ABSTRACT With the exploration of marine resources, the number of underwater nodes is increasing with each passing day, and the demand of mutual cooperative position between nodes is becoming extremely urgent. The existing underwater positioning technology is mainly realized by transplanting cooperative position technology from ground space, without taking into consideration the consequent problems of complex underwater acoustic channels, large signal propagation attenuation and the limited load of underwater nodes. According to the characteristics of the underwater cooperative position network, this paper proposes gaussian parameterized information aided distributed cooperative positioning algorithm (GPI-CP) with underwater environment. The algorithm utilized here is the form of Gauss parameter to calculate information and establish a confidence model. In order to reduce the computational complexity, the Taylor model was adopted to linear approximate European distance. Then distributed underwater node cooperative position is obtained by combing with the factor map theory. This algorithm combined with the sum-product theory and parameterized Gaussian information transmission, is promising to realize fast underwater cooperative position and reduce communication calculations. The proposed algorithm was simulated and analyzed in terms of location ambiguity, ranging error and the number of nodes, etc. When the proposed algorithm was compared with the existing underwater cooperative position method, it was noticed that the position performance had improved more than 10% and the communication calculation is less.

INDEX TERMS Underwater cooperative position, distributed positioning, Gaussian parameter, factor graph.

I. INTRODUCTION

The 21st century is the era of ocean, and the utilization of ocean resources has improved significantly. The multi-node cooperative position and tracking shows advantages at high adaptability, high detection efficiency, and is significantly beneficial in military, and ocean development, etc. Thus, its development has attracted great attention [1]. With the development of underwater communication networks, the research on underwater node positioning technology has become extremely urgent [2]. Earlier underwater positioning technologies were primarily transplanting from wireless communication, such as Direction-of-Arrival Estimation, etc. However, the positioning suffers poor stability due to the high attenuation of underwater electromagnetic waves, the low propagation speed of the commonly used acoustic waves, and the complex underwater environment such as the influence of ocean current and other factors. Also, the positioning accuracy of the single-node DOA estimation was limited, and the information sources were few. Due to large attenuation of electromagnetic waves in water, most underwater detections were realized by transmitting acoustic signals. Besides, the complex underwater environment resulted in excessive reduction of positioning accuracy. It was also difficult to achieve accurate positioning estimates because of poor positioning stability caused by the severe impact of environmental

The associate editor coordinating the review of this manuscript and approving it for publication was Bo Zhang.

This work is licensed under a Creative Commons Attribution 4.0 License. For more information, see https://creativecommons.org/licenses/by/4.0/

factors [3]. In [4], based on the Fourier spectrum estimation, a beam-forming algorithm is proposed, which extends the time domain to the spatial domain. However, the main lobe of the spatial power spectrum of the array signal has a certain width. When two signals with close angles are incident on the receiving array, the main lobe overlaps, which makes it impossible to estimate the Angle-of-Arrival of the signal effectively. Therefore, the condition of effective estimation of the target position is limited by the selection of array spacing. On this basis, the maximum entropy algorithm is proposed in [5], the Capon minimum variance algorithm is proposed in [6] and the Pisarenko harmonic decomposition algorithm is proposed in [7], etc. Although these algorithms improve the azimuth resolution to a certain extent, they have a few shortcomings, such as low efficiency, poor timeliness, etc. In [8], based on the super-resolution theory of subspace decomposition, a multi-signal classification algorithm is proposed. Characteristic decomposition is conducted on the covariance matrix of the target echo signal, and then, the spatial spectrum function is constructed. Through peak search, the signal azimuth can be estimated, and then the specific position of the target can be predicted. This algorithm breaks the limitation of the Fourier spectrum and can recognize the target signal in a single beam. In [9], a rotation-invariant subspace algorithm is proposed. It adopted the rotation invariant property of the subspace of the spatial correlation matrix to directly get the closed-form solution of the angle. Compared with the MUSIC algorithm, this algorithm does not need a spectrum peak search after decomposing the correlation matrix characteristics of array signals. However, there is a certain degree of decline in terms of positioning accuracy and resolution. To overcome this shortcoming, many scholars have proposed several improved algorithms, such as the least square SPRIT algorithm [10]. Besides, there are other DOA estimation algorithms based on subspace, such as the algorithm of maximum likelihood (ML) [11] and the subspace weight algorithm [12]. These algorithms achieve local optimization, but there is still a large amount of computation required.

The above algorithms analyze the cooperative position mainly from the perspective of a single node. In recent years, the main research utilized advanced communications and networking techniques in wireless area to obtain the the mutual ranging information between nodes and realize the cooperative positioning of nodes. In [13], a distributed least squares cooperative position in underwater communication network is proposed. This combines the relaxation of the square distance with the Gauss change information, and then the generalized trust region technology and a two-step location confidence updating process is utilized to simplify the algorithm. The process of updating the algorithm confidence is simple and has low computational complexity but the calculation complexity is large. Also, the introduction of a weight factor significantly improves the positioning accuracy of the algorithm. In [14], a cooperative position algorithm based on semi-definite programming is proposed. By relaxing the non-convex optimization constraints, the cost function minimization is converted to a convex SDP problem. It can achieve better robustness and can guarantee to converge to the global minimum without the optimal initial value. In [15], a cluster location algorithm for wireless sensor networks based on the second-order cone optimization is proposed. It converts the SOCP problem to the global minimization to obtain the location coordinates of the nodes. Thereafter, the Gauss-Newton optimization is adopted to refine the cluster and further improve the positioning accuracy. The algorithms proposed in [14] and [15] are centralized and have high complexity, hence not suitable for large-scale networks. In [16], a hybrid distributed message delivery algorithm based on confidence and average field is proposed. In this algorithm, the confidence is applied in the motion correlation part of the factor graph, and the average field message is used in the measurement correlation part of the factor graph. By using the approximation of Gauss confidence, only three real values are needed for message iteration, which greatly reduce the computational complexity of the algorithm. In [17], a cooperative position algorithm based on connectivity information assisted confidence propagation is proposed. The connectivity information is integrated into the confidence. The unnecessary location information flow is prevented by reducing the location uncertainty occurring in BP-based cooperative position, and the positioning accuracy of the algorithm is improved, however, it is difficult to meet the requirements for the ranging accuracy of communication technology. A distributed cooperative position algorithm based on variation messaging is proposed in [18]. The algorithm utilizes the second-order Taylor expansion to approximate the Gauss form of the nonlinear ranging model, then, only five parameters, the mean value, and covariance of information in the network are transmitted, which significantly reduce the complexity of the algorithm. Prof. Chen proposed a modeling position uncertainty of networked autonomous underwater vehicles and achieve position of underwater autonomous underwater vehicles, but the number of autonomous underwater vehicles is limited and hard to expansion [19]. Prof. Jouhari have research about localization protocols and Internet of Underwater Things, but it also ignore the effect of underwater channel [20]. However, without consideration about the particularity of the underwater acoustic environment, directly application of these algorithms to the underwater cooperative position system results in high complexity, excessive power consumption and the larger interference of underwater wireless communication. In this paper, a distributed underwater cooperative position algorithm based on the Gaussian Parameter - Gaussian Parameter Propagation (GPI-CP) is proposed. Considering the limitation of transmitting power and data rate of underwater cooperative position nodes, the form of Gaussian parameter was adopted to calculate the propagation of information confidence in the network. To reduce multiple extreme points of Gaussian parameter, the non-linear terms in likelihood function were expanded by the first-order Taylor series, so that the expression and transmission of the

confidence information were in the form of Gauss parameter, which were finally combined with factor graph to reduce the influence of interference signal in the channel and realize the underwater node cooperative position. The proposed algorithm has wide application value in intelligent robot swarms such as unmanned underwater vehicles.

II. PROBABILITY DENSITY MODE

In the underwater cooperative node system, due to the random fluctuation of ocean currents and the influence of marine organisms, it is hard to set up the underwater nodes in an underwater suspended environment. Therefore, the existing co-location method based on Gaussian distribution distance measurement is not suitable for underwater co-location. In this paper, a confidence propagation model based on factor graph is proposed to describe the position change of underwater cooperative nodes adaptively. This algorithm can well reflect the influence of communication ranging error caused by underwater multipath interference and propagation error caused by signal attenuation on the positioning results of underwater nodes.

In practice, the underwater nodes working in long term are anchored along the seabed to sustain high stability. Therefore, in the underwater node cooperative position system designed in this paper, the two-dimensional plane was adopted to realize the positioning, and the height information was corrected by the water pressure gauge and seabed mapping data and the height measurement method is proposed in [20]. In the underwater cooperative node network system, the underwater nodes with high stability were selected as anchor nodes. The positioning data of anchor nodes was accurately known, and the remaining underwater nodes were treated as the nodes to be positioned. Consider an underwater cooperative network which includes M anchor nodes and N nodes to be positioned. Let $\mathcal{M}$ represents the set of all anchor nodes, $\mathcal{N}$ represents the set of all nodes to be positioned, and S represents the set of all nodes in the network. Then $S = \mathcal{M} \cup \mathcal{N}$. Denote the coordinate of node i as $\mathbf{x}_i = [x_i, y_i]$. Then $\mathbf{X} = \{\mathbf{x}_i | i \in S\}$ represents the set of all node locations. Define $\mathcal{M}_i$ and $\mathcal{N}_i$ as the set of neighbor anchor nodes and the set of neighbor undetermined nodes for node i, respectively. Then $S_i = \mathcal{M}_i \cup \mathcal{N}_i$ includes all the neighbor nodes for node i in the network.

The cooperative network of underwater nodes is set as follows.

1) the communication distance equals to the measurement distance, which is set as R.
2) the ranging information error between node i and node j follows Gaussian distribution, i.e. $n_{j\to i} \sim N\left(0, \sigma_{ij}^2\right)$.
3) the prior probability $p(\mathbf{x}_i)$ of all the nodes is independent, and the prior probability of the x-axis and y-axis $p(x_i), p(y_i)$, are independent also.

In this way, the ranging at undetermined node i to any of its neighbor nodes $j \in S_i$ can be expressed as:

$$z_{j\to i} = \left\|\mathbf{x}_j - \mathbf{x}_i\right\| + n_{j\to i} \tag{1}$$

where $\|\cdot\|$ represents Euclidean norm. Define $\mathbf{Z}_i = \left\{z_{j\to i} | j \in S_i\right\}$ as the set of ranging information of undetermined node i to all of its neighbor nodes, and $\mathbf{Z} = \{\mathbf{Z}_i | i \in \mathcal{N}_i\}$ is the set of ranging information of all the undetermined nodes in the network. With the location information $\mathbf{x}_i$ and $\mathbf{x}_j$, the likelihood function of the ranging $p\left(z_{j\to i} | \mathbf{x}_i, \mathbf{x}_j\right)$ is expressed as

$$p\left(z_{j\to i} | \mathbf{x}_i, \mathbf{x}_j\right) = \frac{1}{\sqrt{2\pi\sigma_{ij}^2}} \exp\left\{-\frac{(z_{j\to i} - \left\|\mathbf{x}_i - \mathbf{x}_j\right\|)^2}{2\sigma_{ij}^2}\right\} \tag{2}$$

According to the principle of Bayesian estimation, to get the estimation of location $\boldsymbol{x}_i$, we need to get the posterior probability $p(\mathbf{x}_i | \mathbf{Z})$ first, and then the minimum mean square error estimation (MMSE) is adopt to update the position error and achieve initial position estimation:

$$\hat{\mathbf{x}}_i = \int \mathbf{x}_i{}^* p(\mathbf{x}_i | \mathbf{Z}) d\mathbf{x}_i \tag{3}$$

The location posterior probability of undetermined node i can be acquired by the marginal integral of joint posterior probability distribution $p(\mathbf{X} | \mathbf{Z})$ as:

$$p(\mathbf{x}_i | \mathbf{Z}) = \int p(\mathbf{X} | \mathbf{Z}) d\mathbf{X} \backslash \mathbf{x}_i \tag{4}$$

where $d\mathbf{X}\backslash\mathbf{x}_i$ represents all variables in X collection except variable $\mathbf{x}_i$. Assume independence of the statistical characteristics among nodes, we can get:

$$p(\mathbf{X} | \mathbf{Z}) \propto p(\mathbf{Z} | \mathbf{X}) p(\mathbf{X}) = \prod_{i\in\mathcal{N}} \left(\prod_{j\in S_i} p\left(z_{j\to i} \middle| \mathbf{x}_j, \mathbf{x}_i\right)\right) \times \prod_{i\in\mathcal{N}} p(\mathbf{x}_i) \prod_{a\in\mathcal{M}} p(\mathbf{x}_a) \tag{5}$$

where $p(\mathbf{x}_i)$ and $p(\mathbf{x}_a)$ represent the prior probability distribution of function nodes and anchor nodes respectively.

III. UNDERWATER DISTRIBUTED COOPERATIVE POSITION METHOD

Since the factor graph theory can replace the optimal value of the global variable by the product of the optimal value of the local variables in the underwater cooperative position network, the discontinuity and uncertainty of the underwater node communication, the positioning performance of the whole underwater distributed cooperative node network can be improved by the product of the local cooperative position of single underwater node. In this paper, a typical underwater network topology as shown in Figure 1 with four underwater nodes was studied. The gray nodes denote anchor nodes with known location and high coordinate accuracy, while the white nodes are undetermined nodes. When node 2 was located, node 4 was also known as the cooperative node of node 2.

From the general conclusion of Equation (5), the joint posterior probability distribution of all node position variables

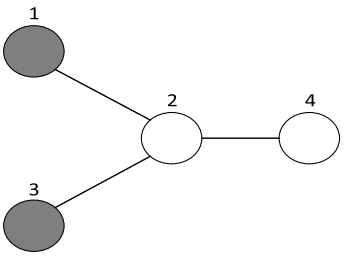

FIGURE 1. Typical underwater network topology.

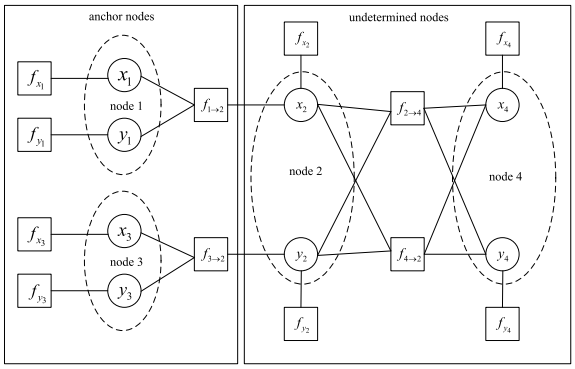

FIGURE 2. Combined posterior probability factor graph.

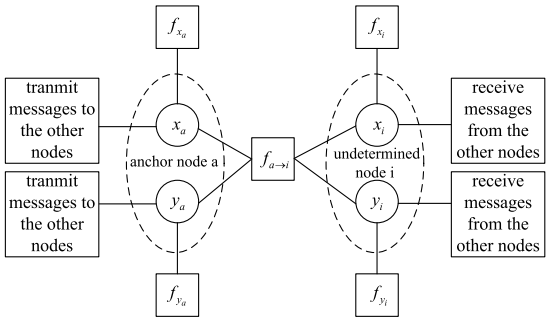

(a) local factor graph between anchor nodes and undetermined nodes

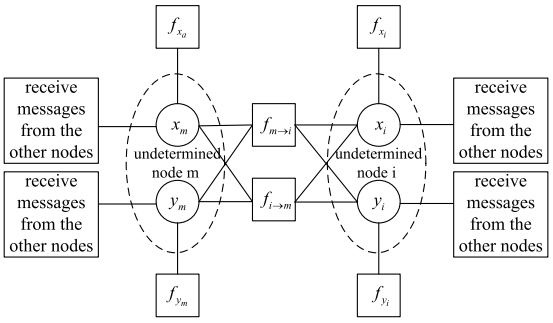

(b) local factor graph between undetermined nodes

FIGURE 3. Two kinds of sub-factor graph structures.

in Figure 1 is shown as follows:

$$\begin{aligned} p\left(\mathbf{X}\,|\mathbf{Z}\right) &= p(\mathbf{x}_1, \mathbf{x}_2, \mathbf{x}_3, \mathbf{x}_4\,|z_{1\to 2}\,, z_{3\to 2}, z_{4\to 2}) \\ &= p(z_{1\to 2}|\mathbf{x}_1, \mathbf{x}_2,)p(z_{3\to 2}|\mathbf{x}_2, \mathbf{x}_3) \\ &\quad \times p(z_{4\to 2}|\mathbf{x}_2, \mathbf{x}_4)p(\mathbf{x}_1)p(\mathbf{x}_2)p(\mathbf{x}_3)p(\mathbf{x}_4) \end{aligned} \tag{6}$$

where $\mathbf{x}_i = [x_i, y_i]$ denotes the coordinates of node i; $f_{x_i} = p\left(x_i\right), f_{y_i} = p\left(y_i\right)$ represent the prior probability of node position on x-axis and y-axis;$f_{j\to k} = p\left(z_{j\to k}|\mathbf{x}_j, \mathbf{x}_k\right)$ represents the likelihood function of the ranging information. The factor graph of Equation (6) is shown as Figure 2.

As seen from Figure 2, the scale of the factor graph depends on the topology size of the underwater cooperative network. It can effectively reduce the interference of underwater acoustic channel. A large number of underwater nodes will lead to a complex structure of the joint posterior probability factor graph. For any undetermined node, the joint posterior probability factor graph included two sub-factor graph structures. One was a sub-graph composed of information from the anchor nodes, as shown in Figure 3(a), and the other was a sub-graph composed of information from the cooperative nodes (neighbor nodes to be positioned), as shown in Figure 3(b). Anchor nodes could provide information for neighbor nodes, but request no information back, there is only likelihood function $f_{a\to i}$(factor nodes) of ranging information from anchor nodes to undetermined nodes. As the information between the undetermined nodes was mutually exchangeable, there existed two factor nodes $f_{m\to i}$ and $f_{i\to m}$ as shown in Figure 3(b).

As seen from Figure 3, for each undetermined node, there were two types of information: input information from other function nodes and output information transmitted to other function nodes.

A. INFORMATION REPRESENTATIONS

(1)Input information

For anchor node *a*:

Assume the location of the anchor node was not updated, only provided information for neighbor nodes, that is, only output information and no input information.

For undetermined node *i*:

The undetermined nodes first received information from the neighbor nodes (including anchor nodes and cooperative nodes) and updated the principles through factor graph and information from function node to variable node in product theory. For undetermined node i in the lth iteration, the input information from the function node $f_{a\to i}$ in Figure 3(a) are expressed as:

$$\mu^{(l)}_{f_{a\to i}\to x_i} = \iiint f_{a\to i}\mu^{(l-1)}_{\mathbf{x}_a\to f_{a\to i}}\mu^{(l-1)}_{y_i\to f_{a\to i}}d\mathbf{x}_a dy_i \tag{7}$$

$$\mu^{(l)}_{f_{a\to i}\to y_i} = \iiint f_{a\to i}\mu^{(l-1)}_{\mathbf{x}_a\to f_{a\to i}}\mu^{(l-1)}_{x_i\to f_{a\to i}}d\mathbf{x}_a dx_i \tag{8}$$

Similarly, the input information from function nodes $f_{m\to i}$ and $f_{i\to m}$ in Figure 3(b)is expressed as:

$$\mu^{(l)}_{f_{m\to i}\to x_i} = \iiint f_{m\to i}\mu^{(l-1)}_{\mathbf{x}_m\to f_{m\to i}}\mu^{(l-1)}_{y_i\to f_{m\to i}}d\mathbf{x}_m dy_i \tag{9}$$

$$\mu^{(l)}_{f_{m\to i}\to y_i} = \iiint f_{m\to i}\mu^{(l-1)}_{\mathbf{x}_m\to f_{m\to i}}\mu^{(l-1)}_{x_i\to f_{m\to i}}d\mathbf{x}_m dx_i \tag{10}$$

$$\mu^{(l)}_{f_{i\to m}\to x_m} = \iiint f_{i\to m}\mu^{(l-1)}_{\mathbf{x}_i\to f_{m\to i}}\mu^{(l-1)}_{y_m\to f_{i\to m}} d\mathbf{x}_i dy_m \quad (11)$$

$$\mu^{(l)}_{f_{i\to m}\to y_m} = \iiint f_{i\to m}\mu^{(l-1)}_{\mathbf{x}_i\to f_{i\to m}}\mu^{(l-1)}_{x_m\to f_{i\to m}} d\mathbf{x}_i dx_m \quad (12)$$

In these equations, $\mu^{(l-1)}_{x_m\to f_{m\to i}}$, $\mu^{(l-1)}_{y_m\to f_{m\to i}}$, $\mu^{(l-1)}_{x_m\to f_{i\to m}}$, $\mu^{(l-1)}_{y_m\to f_{i\to m}}$ represent the output information at $l-1th$ of the neighbor node m, $\mu^{(l-1)}_{x_i\to f_{m\to i}}$, $\mu^{(l-1)}_{y_i\to f_{m\to i}}$, $\mu^{(l-1)}_{x_i\to f_{i\to m}}$, $\mu^{(l-1)}_{y_i\to f_{i\to m}}$ represent the output information at $l-1th$ of the node i to be located.

B. CONFIDENCE MODEL

By receiving information from all function nodes, the edge posterior probability distribution (confidence) of variable nodes $\boldsymbol{x}_i$ was updated as follows:

$$\begin{aligned} b^{(l)}(x_i) &= p(x_i|\mathbf{Z}) \\ &= f_{x_i}\prod_{j\in\mathcal{N}_i}\left[\mu^{(l)}_{f_{j\to i}\to x_i}\mu^{(l)}_{f_{i\to j}\to x_i}\right]\prod_{k\in\mathcal{M}_i}\mu^{(l)}_{f_{k\to i}\to x_i} \end{aligned} \quad (13)$$

$$\begin{aligned} b^{(l)}(y_i) &= p(y_i|\mathbf{Z}) \\ &= f_{y_i}\prod_{j\in\mathcal{N}_i}\left[\mu^{(l)}_{f_{j\to i}\to x_i}\mu^{(l)}_{f_{i\to j}\to y_i}\right]\prod_{k\in\mathcal{M}_i}\mu^{(l)}_{f_{k\to i}\to y_i} \end{aligned} \quad (14)$$

C. LOCATION ESTIMATION OF UNDETERMINED NODES

The position estimation of undetermined node i was obtained by MMSE calculation, which is shown as follows:

$$\hat{x}^{(l)}_i = \int x_i p(x_i|\mathbf{Z})\,dx_i = \int x_i b^{(l)}(x_i)\,dx_i \quad (15)$$

$$\hat{y}^{(l)}_i = \int y_i p(y_i|\mathbf{Z})\,dy_i = \int y_i b^{(l)}(y_i)\,dy_i \quad (16)$$

D. OUTPUT INFORMATION

For anchor node a:

Due to the high positioning accuracy and known location information of anchor nodes and interference of underwater channel is larger, the information from anchor nodes was considered as Dikela δ function, so we get the following:

$$\mu^{(l-1)}_{x_a\to f_{a\to i}} = f_{x_a} = \delta\left(x_a - m_{x_a}\right) \quad (17)$$

$$\mu^{(l-1)}_{y_a\to f_{a\to i}} = f_{y_a} = \delta\left(y_a - m_{y_a}\right) \quad (18)$$

where m_{x_a} and m_{y_a} represent the location of anchor nodes on x-axis and y-axis, respectively.

For undetermined node i:

The output information of each undetermined node was used for the next iteration. According to the sum-product theory of factor graph, the output information from variable nodes x_i and y_i to function node $f_{a\to i}$ in Figure 3(a) can be expressed as

$$\begin{aligned} \mu^{(l)}_{x_i\to f_{a\to i}} &= f_{x_i}\prod_{j\in\mathcal{N}_i}\left[\mu^{(l)}_{f_{j\to i}\to x_i}\mu^{(l)}_{f_{i\to j}\to x_i}\right]\prod_{k\in\{\mathcal{M}_i\setminus a\}}\mu^{(l)}_{f_{k\to i}\to x_i} \\ &= \frac{b^{(l)}(x_i)}{\mu^{(l)}_{f_{a\to i}\to x_i}} \end{aligned} \quad (19)$$

$$\begin{aligned} \mu^{(l)}_{y_i\to f_{a\to i}} &= f_{y_i}\prod_{j\in\mathcal{N}_i}\left[\mu^{(l)}_{f_{j\to i}\to y_i}\mu^{(l)}_{f_{i\to j}\to x_i}\right]\prod_{k\in\{\mathcal{M}_i\setminus a\}}\mu^{(l)}_{f_{k\to i}\to y_i} \\ &= \frac{b^{(l)}(y_i)}{\mu^{(l)}_{f_{a\to i}\to y_i}} \end{aligned} \quad (20)$$

As can be seen from Equation (19-20) that variable nodes x_i and y_i send different information to their neighbor function nodes, which is of great complexity and communication load. In fact, because of the cycle in the factor graph model, confidence was an approximate inference algorithm which implies that adding or reducing an option $\mu^{(l)}_{x_i\to f_{a\to i}}$, $\mu^{(l)}_{y_i\to f_{a\to i}}$ did not improve or degrade the performance. Therefore, the output information can be approximated by the confidence of variable nodes as

$$\mu^{(l)}_{x_i\to f_{a\to i}} = b^{(l)}(x_i) \quad (21)$$

$$\mu^{(l)}_{y_i\to f_{a\to i}} = b^{(l)}(y_i) \quad (22)$$

Similarly, the information from variable nodes x_i and y_i to function nodes $f_{m\to i}$ and $f_{i\to m}$ in Figure 3(b) can be expressed as:

$$\mu^{(l)}_{x_i\to f_{m\to i}} = \frac{b^{(l)}(x_i)}{\mu^{(l)}_{f_{m\to i}\to x_i}} = b^{(l)}(x_i) \quad (23)$$

$$\mu^{(l)}_{y_i\to f_{m\to i}} = \frac{b^{(l)}(y_i)}{\mu^{(l)}_{f_{m\to i}\to y_i}} = b^{(l)}(y_i) \quad (24)$$

$$\mu^{(l)}_{x_i\to f_{i\to m}} = \frac{b^{(l)}(x_i)}{\mu^{(l)}_{f_{i\to m}\to x_i}} = b^{(l)}(x_i) \quad (25)$$

$$\mu^{(l)}_{y_i\to f_{i\to m}} = \frac{b^{(l)}(y_i)}{\mu^{(l)}_{f_{i\to m}\to y_i}} = b^{(l)}(y_i) \quad (26)$$

As can be seen from Equation (21-26), the output information from one variable node to all of its neighbor function nodes is equal, which is broadcast information of their confidence to all neighbor nodes, which in turn reduces calculation burden.

E. INFORMATION PARAMETERIZATION

Although the prior probabilities of variables x_i and y_i were initialized to Gaussian distribution, the information in the factor graph was generally not in Gaussian form, because the ranging function was a non-linear Euclidean distance. In this paper, the first-order Taylor series was utilized to expand the non-linear term of the approximate likelihood function, so that the closed Gaussian information expression could be obtained.

Information from the function node $f_{a\to i}$

Suppose that at $l-1th$ iteration, the information $\mu_{x_i\to f_{a\to i}}^{(l-1)}$, $\mu_{y_i\to f_{a\to i}}^{(l-1)}$ follows Gaussian distribution. Substituting Equation (2) into (7), we get:

$$\mu_{f_{a\to i}\to x_i}^{(l)} \propto \int \frac{1}{\sqrt{2\pi}\sigma_{a\to i}} \exp\left\{-\frac{\left(z_{a\to i}-\left\|\mathbf{m}_{x_a}-\mathbf{x}_i\right\|\right)^2}{2\sigma_{a\to i}^2}\right\} \times N\left(y_i, m_{y_i\to f_{a\to i}}^{(l-1)}, \left(\sigma_{y_i\to f_{a\to i}}^{(l-1)}\right)^2\right) dy_i \tag{27}$$

Expand the non-linear term in Equation(27) by the first-order Taylor series at the $l-1th$ iterative coordinate estimate $\left(\hat{x}_i^{(l-1)}, \hat{y}_i^{(l-1)}\right)$, that is:

$$\left\|\mathbf{m}_{x_a}-\mathbf{x}_i\right\| = \hat{d}_{a\to i}^{(l-1)} + \frac{\hat{x}_i^{(l-1)}-m_{x_a}}{\hat{d}_{a\to i}^{(l-1)}}\left(x_i-\hat{x}_i^{(l-1)}\right) + \frac{\hat{y}_i^{(l-1)}-m_{y_a}}{\hat{d}_{a\to i}^{(l-1)}}\left(y_i-\hat{y}_i^{(l-1)}\right) \tag{28}$$

where $\hat{d}_{a\to i}^{(l-1)} = \left\|\mathbf{m}_{x_a}-\hat{\mathbf{x}}_i^{(l-1)}\right\|$. Substituting equation (28) by equation (29), we get:

$$\mu_{f_{a\to i}\to x_i}^{(l)} \propto N\left(x_i, m_{x_a} + z_{a\to i}\frac{\hat{x}_i^{(l-1)}-m_{x_a}}{\hat{d}_{a\to i}^{(l-1)}}, \sigma_{a\to i}^2\right) \tag{29}$$

Similarly, it can be calculated that:

$$\mu_{f_{a\to i}\to y_i}^{(l)} \propto N\left(y_i, m_{y_a} + z_{a\to i}\frac{\hat{y}_i^{(l-1)}-m_{y_a}}{\hat{d}_{a\to i}^{(l-1)}}, \sigma_{a\to i}^2\right) \tag{30}$$

Information from function nodes $f_{m\to i}$ and $f_{i\to m}$

Suppose that at $l-1th$ iteration, the information $\mu_{x_m\to f_{m\to i}}^{(l-1)}$, $\mu_{y_m\to f_{m\to i}}^{(l-1)}$, $\mu_{y_i\to f_{m\to i}}^{(l-1)}$ follows Gaussian distribution. Substituting Equation (2) by (29), Denote the coordinate of node m as $\mathbf{x}_m=[x_m, y_m]$.we get:

$$\mu_{f_{m\to i}\to x_i}^{(l)} \propto \iiint \frac{1}{\sqrt{2\pi}\sigma_{m\to i}} \times \exp\left\{-\frac{\left(z_{m\to i}-\left\|\mathbf{m}_{x_m}-\mathbf{x}_i\right\|\right)^2}{2\sigma_{m\to i}^2}\right\} \times N\left(\mathbf{x}_m, m_{\mathbf{x}_m\to f_{m\to i}}^{(l-1)}, \left(\sigma_{\mathbf{x}_m\to f_{m\to i}}^{(l-1)}\right)^2\right) \times N\left(y_i, m_{y_i\to f_{m\to i}}^{(l-1)}, \left(\sigma_{y_i\to f_{m\to i}}^{(l-1)}\right)^2\right) d\mathbf{x}_m dy_i \tag{31}$$

Expand the nonlinear term in Equation(31) by the first-order Taylor series at the $l-1th$ iterative coordinate estimate $\left(\hat{x}_i^{(l-1)}, \hat{y}_i^{(l-1)}\right)$, and $\left(\hat{x}_m^{(l-1)}, \hat{y}_m^{(l-1)}\right)$, that is:

$$\left\|\mathbf{m}_{x_m}-\mathbf{x}_i\right\| = \hat{d}_{m\to i}^{(l-1)} + \frac{\hat{\mathbf{x}}_i^{(l-1)}-\hat{\mathbf{x}}_m^{(l-1)}}{\hat{d}_{m\to i}^{(l-1)}}\left(\mathbf{x}_i-\hat{\mathbf{x}}_i^{(l-1)}\right) + \frac{\hat{\mathbf{x}}_m^{(l-1)}-\hat{\mathbf{x}}_i^{(l-1)}}{\hat{d}_{m\to i}^{(l-1)}}\left(\mathbf{x}_m-\hat{\mathbf{x}}_m^{(l-1)}\right) \tag{32}$$

where $\hat{d}_{m\to i}^{(l-1)} = \left\|m_{\mathbf{x}_m}-\hat{\mathbf{x}}_i^{(l-1)}\right\|$. Substituting equation (32) by equation (31), we get:

$$\mu_{f_{m\to i}\to x_i}^{(l)} \propto N\left(x_i, m_{x_m\to f_{m\to i}}^{(l-1)} + z_{m\to i}\frac{\hat{x}_i^{(l-1)}-\hat{x}_m^{(l-1)}}{\hat{d}_{m\to i}^{(l-1)}}, \times \sigma_{m\to i}^2 + \left(\sigma_{x_m\to f_{m\to i}}^{(l-1)}\right)^2\right) \tag{33}$$

Similarly, it can be calculated that:

$$\mu_{f_{m\to i}\to y_i}^{(l)} \propto N\left(y_i, m_{y_m\to f_{m\to i}}^{(l-1)} + z_{m\to i}\frac{\hat{y}_i^{(l-1)}-\hat{y}_m^{(l-1)}}{\hat{d}_{m\to i}^{(l-1)}}, \times \sigma_{m\to i}^2 + \left(\sigma_{y_m\to f_{m\to i}}^{(l-1)}\right)^2\right) \tag{34}$$

$$\mu_{f_{i\to m}\to x_i}^{(l)} \propto N\left(x_i, m_{x_m\to f_{i\to m}}^{(l-1)} + z_{i\to m}\frac{\hat{x}_i^{(l-1)}-\hat{x}_m^{(l-1)}}{\hat{d}_{i\to m}^{(l-1)}}, \times \sigma_{i\to m}^2 + \left(\sigma_{x_m\to f_{i\to m}}^{(l-1)}\right)^2\right) \tag{35}$$

$$\mu_{f_{i\to m}\to y_i}^{(l)} \propto N\left(y_i, m_{y_m\to f_{i\to m}}^{(l-1)} + z_{i\to m}\frac{\hat{y}_i^{(l-1)}-\hat{y}_m^{(l-1)}}{\hat{d}_{i\to m}^{(l-1)}}, \times \sigma_{i\to m}^2 + \left(\sigma_{y_m\to f_{i\to m}}^{(l-1)}\right)^2\right) \tag{36}$$

Then the confidence of undetermined node i is calculated as follows:

$$b^{(l)}(x_i) \propto N\left(x_i, m_{x_i}^{(l)}, \left(\sigma_{x_i}^{(l)}\right)^2\right) \tag{37}$$

$$b^{(l)}(y_i) \propto N\left(y_i, m_{y_i}^{(l)}, \left(\sigma_{y_i}^{(l)}\right)^2\right) \tag{38}$$

The mean and variance are updated as:

$$m_{x_i}^{(l)} = \frac{m_{x_i}^{(0)}\left(\sigma_{x_i}^{(l)}\right)^2}{\left(\sigma_{x_i}^{(0)}\right)^2} + \left(\sigma_{x_i}^{(l)}\right)^2 \sum_{k\in\mathcal{M}_i}\frac{m_{f_{k\to i}\to x_i}^{(l)}}{\left(\sigma_{f_{k\to i}\to x_i}^{(l)}\right)^2} + \left(\sigma_{x_i}^{(l)}\right)^2 \sum_{j\in\mathcal{N}_i}\left[\frac{m_{f_{j\to i}\to x_i}^{(l)}}{\left(\sigma_{f_{j\to i}\to x_i}^{(l)}\right)^2} + \frac{m_{f_{i\to j}\to x_i}^{(l)}}{\left(\sigma_{f_{i\to j}\to x_i}^{(l)}\right)^2}\right] \tag{39}$$

$$m_{y_i}^{(l)} = \frac{m_{y_i}^{(0)}\left(\sigma_{y_i}^{(l)}\right)^2}{\left(\sigma_{y_i}^{(0)}\right)^2} + \left(\sigma_{y_i}^{(l)}\right)^2 \sum_{k\in\mathcal{M}_i} \frac{m_{f_{k\to i}\to y_i}^{(l)}}{\left(\sigma_{f_{k\to i}\to y_i}^{(l)}\right)^2} + \left(\sigma_{y_i}^{(l)}\right)^2 \sum_{j\in\mathcal{N}_i} \left[\frac{m_{f_{j\to i}\to y_i}^{(l)}}{\left(\sigma_{f_{j\to i}\to y_i}^{(l)}\right)^2} + \frac{m_{f_{i\to j}\to y_i}^{(l)}}{\left(\sigma_{f_{i\to j}\to y_i}^{(l)}\right)^2} \right] \tag{40}$$

$$\frac{1}{\left(\sigma_{x_i}^{(l)}\right)^2} = \frac{1}{\left(\sigma_{x_i}^{(0)}\right)^2} + \sum_{k\in\mathcal{M}_i} \frac{1}{\left(\sigma_{f_{k\to i}\to x_i}^{(l)}\right)^2} + \sum_{j\in\mathcal{N}_i} \left[\frac{1}{\left(\sigma_{f_{j\to i}\to x_i}^{(l)}\right)^2} + \frac{1}{\left(\sigma_{f_{i\to j}\to x_i}^{(l)}\right)^2} \right] \tag{41}$$

$$\frac{1}{\left(\sigma_{y_i}^{(l)}\right)^2} = \frac{1}{\left(\sigma_{y_i}^{(0)}\right)^2} + \sum_{k\in\mathcal{M}_i} \frac{1}{\left(\sigma_{f_{k\to i}\to y_i}^{(l)}\right)^2} + \sum_{j\in\mathcal{N}_i} \left[\frac{1}{\left(\sigma_{f_{j\to i}\to y_i}^{(l)}\right)^2} + \frac{1}{\left(\sigma_{f_{i\to j}\to y_i}^{(l)}\right)^2} \right] \tag{42}$$

It's plausible to suppose that $m_{f_{j\to i}\to x_i}^{(l)} = m_{f_{i\to j}\to x_i}^{(l)}$ and $\left(\sigma_{f_{j\to i}\to x_i}^{(l)}\right)^2 = \left(\sigma_{f_{i\to j}\to x_i}^{(l)}\right)^2$. Then the Equation(39-42) can be simplified as:

$$m_{x_i}^{(l)} = \frac{m_{x_i}^{(0)}\left(\sigma_{x_i}^{(l)}\right)^2}{\left(\sigma_{x_i}^{(0)}\right)^2} + \left(\sigma_{x_i}^{(l)}\right)^2 \sum_{j\in\mathcal{N}_i} \frac{2m_{f_{j\to i}\to x_i}^{(l)}}{\left(\sigma_{f_{j\to i}\to x_i}^{(l)}\right)^2} + \left(\sigma_{x_i}^{(l)}\right)^2 \sum_{k\in\mathcal{M}_i} \frac{m_{f_{k\to i}\to x_i}^{(l)}}{\left(\sigma_{f_{k\to i}\to x_i}^{(l)}\right)^2} \tag{43}$$

$$m_{y_i}^{(l)} = \frac{m_{y_i}^{(0)}\left(\sigma_{y_i}^{(l)}\right)^2}{\left(\sigma_{y_i}^{(0)}\right)^2} + \left(\sigma_{y_i}^{(l)}\right)^2 \sum_{j\in\mathcal{N}_i} \frac{2m_{f_{j\to i}\to y_i}^{(l)}}{\left(\sigma_{f_{j\to i}\to y_i}^{(l)}\right)^2} + \left(\sigma_{y_i}^{(l)}\right)^2 \sum_{k\in\mathcal{M}_i} \frac{m_{f_{k\to i}\to y_i}^{(l)}}{\left(\sigma_{f_{k\to i}\to y_i}^{(l)}\right)^2} \tag{44}$$

$$\frac{1}{\left(\sigma_{x_i}^{(l)}\right)^2} = \frac{1}{\left(\sigma_{x_i}^{(0)}\right)^2} + \sum_{j\in\mathcal{N}_i} \frac{2}{\left(\sigma_{f_{j\to i}\to x_i}^{(l)}\right)^2} + \sum_{k\in\mathcal{M}_i} \frac{1}{\left(\sigma_{f_{k\to i}\to x_i}^{(l)}\right)^2} \tag{45}$$

$$\frac{1}{\left(\sigma_{y_i}^{(l)}\right)^2} = \frac{1}{\left(\sigma_{y_i}^{(0)}\right)^2} + \sum_{j\in\mathcal{N}_i} \frac{2}{\left(\sigma_{f_{j\to i}\to y_i}^{(l)}\right)^2} + \sum_{k\in\mathcal{M}_i} \frac{1}{\left(\sigma_{f_{k\to i}\to y_i}^{(l)}\right)^2} \tag{46}$$

IV. ALGORITHM PROCESS

The steps of the distributed underwater cooperative position algorithm based on parameterized Gaussian information are given in Table 1. We note that it included two stages: initialization and loop iteration. The initial positioning information of all nodes is their initial water entry positioning information.

TABLE 1. Algorithmic representation: GPI-CP.

1 Initialization

1) For the anchor nodes $a \in \mathcal{M}$, set the prior information as

$$f_{x_a}(x_a) = \delta\left(x_a - m_{x_a}\right), f_{y_a}(y_a) = \delta\left(y_a - m_{y_a}\right)$$

2) For all the undetermined nodes $i \in \mathcal{N}$, the prior information as

$$f_{x_i}(x_i) = N\left(x_i, m_{x_i}^{(0)}, \left(\sigma_{x_i}^{(0)}\right)^2\right)$$

$$f_{y_i}(y_i) = N\left(y_i, m_{y_i}^{(0)}, \left(\sigma_{y_i}^{(0)}\right)^2\right)$$

3) For all the nodes in the network, Broadcasting its own location.

4) For all the undetermined nodes

b1) Receiving location information from neighbor underwater nodes

b2) Measuring the distance $z_{j\to i}$ with neighbor underwater nodes, and the variance $\sigma_{j\to i}^2 (i \in S_i)$ of ranging error

2 Iterative loop

For all the undetermined nodes

While (iteration index<preset maximum number)

c1)calculating input information $\mu_{f_{a\to i}\to x_i}^{(l)}$, $\mu_{f_{a\to i}\to y_i}^{(l)}$, $\mu_{f_{m\to i}\to x_i}^{(l)}$, $\mu_{f_{m\to i}\to y_i}^{(l)}$, $\mu_{f_{i\to m}\to x_i}^{(l)}$ and $\mu_{f_{i\to m}\to y_i}^{(l)}$.

c2)calculating the mean values $m_{x_i}^{(l)}$, $m_{y_i}^{(l)}$ and variances $\left(\sigma_{x_i}^{(l)}\right)^2$, $\left(\sigma_{y_i}^{(l)}\right)^2$ of location confidence of the nodes to be positioned.

c3)computing the output information $\mu_{x_i\to f_{a\to i}}^{(l)}$, $\mu_{y_i\to f_{a\to i}}^{(l)}$, $\mu_{x_i\to f_{m\to i}}^{(l)}$, $\mu_{y_i\to f_{m\to i}}^{(l)}$, $\mu_{x_i\to f_{i\to m}}^{(l)}$ and $\mu_{y_i\to f_{i\to m}}^{(l)}$。

end

Calculating the location of all underwater nodes $i \in \mathcal{N}$ to be positioned according to MMSE.

V. SIMULATION RESULTS AND ANALYSIS

In the simulation part, the positioning performance of GPI-CP distributed underwater cooperative position algorithm was simulated and analyzed. In the simulation, a $10\times10km^2$ cooperative underwater positioning network area including M anchor nodes and N undetermined nodes was set up. In the network area, the anchor nodes were the underwater

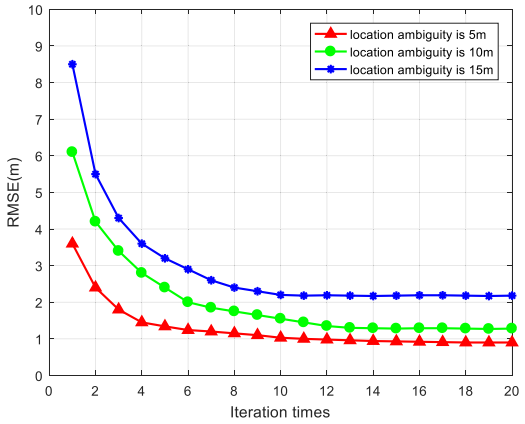

FIGURE 4. Positioning performance under different location ambiguities(RMSE).

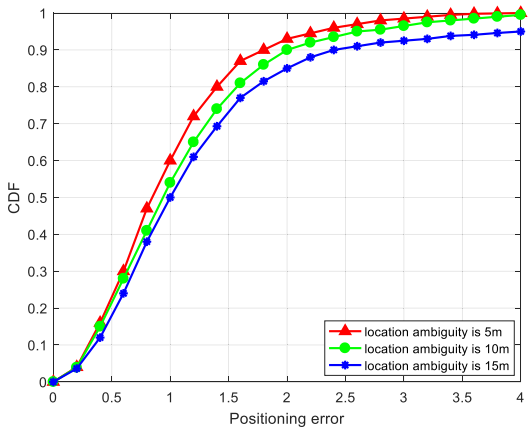

FIGURE 5. Positioning performance under different location ambiguities (CDF).

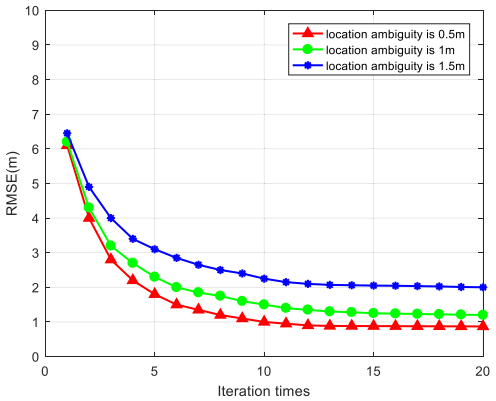

FIGURE 6. Positioning performance under different ranging errors (RMSE).

nodes with high positioning accuracy, and their positions were set unchanged. The undetermined nodes were randomly and evenly distributed in the cooperative location network plane, and the communication distance between each underwater node was same with the ranging R and obtained by asynchronous measurements method [21]. It is assumed that the ranging noise between any two underwater nodes obeyed the Gaussian white noise with mean value of 0 and variance of $\sigma^2_{j\to i}$. The prior position probability distribution of the undetermined node i on the x-axis and y-axis is respectively as follows:

$$f_{x_i}(x_i) = N\left(x_i, m^{(0)}_{x_i}, \left(\sigma^{(0)}_{x_i}\right)^2\right) \tag{47}$$

$$f_{y_i}(y_i) = N\left(y_i, m^{(0)}_{y_i}, \left(\sigma^{(0)}_{y_i}\right)^2\right) \tag{48}$$

In the simulation, assuming $\sigma^{(0)}_{x_i} = \sigma^{(0)}_{y_i} = \sigma_p$; the maximum time of iteration was set as L $= 20$ times; the Monte Carlo time was set as T. The positioning performance of the algorithm was simulated and analyzed from four aspects, such as position ambiguity, ranging error, location node scale and communication calculation. The test was conducted in a water tank environment.

A. EFFECT OF POSITION AMBIGUITY

The influence of the ambiguity of prior position information of underwater nodes on convergence speed and positioning accuracy was analyzed in Figure 4 and 5. The simulation parameters were: number of anchor nodes $M = 13$, number of undetermined nodes $N = 100$. The standard deviation of ranging noise was 1m, and the Monte Carlo simulation time was T $= 500$ times.

As can be seen from Figure 5, the positioning accuracy of underwater nodes gradually increased with the decrease of position ambiguity. This is because prior information provided by the neighbor nodes is more accurate with low σ_p. It can also be seen from Figure 4 that low σ_p lead to fast convergence. This is because with accurate prior position information, the first-order Taylor series would expand close to the real position of the undetermined nodes, thus speeding up the convergence.

B. THE EFFECT OF RANGING ERROR

The effect of the standard deviation of ranging error on convergence speed and positioning accuracy was analyzed in Figure 6 and 7, respectively. The number of anchor nodes $M = 13$, the number of undetermined nodes $N = 100$. The standard deviation of prior information location ambiguity of the nodes was 10m, and the Monte Carlo simulation time was T $= 500$ times.

It can be seen from Figure 6 and 7 that with the decrease of the standard deviation of ranging error, the positioning accuracy of the underwater nodes increased accordingly. This is because the smaller the standard deviation of ranging error, the closer is the measurement distance between the undetermined nodes and the neighbor nodes in comparison to the real distance between them. Further, the more reliable the underwater cooperative information provided by the neighbor nodes to the undetermined nodes, the better is the positioning performance of underwater nodes.

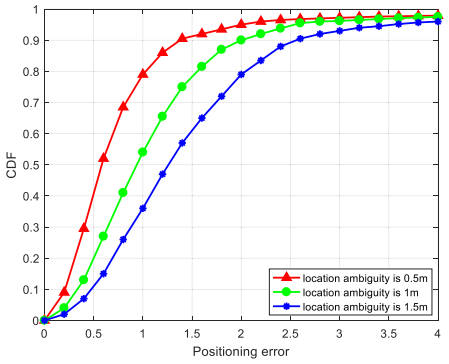

FIGURE 7. Positioning performance under different ranging errors (CDF).

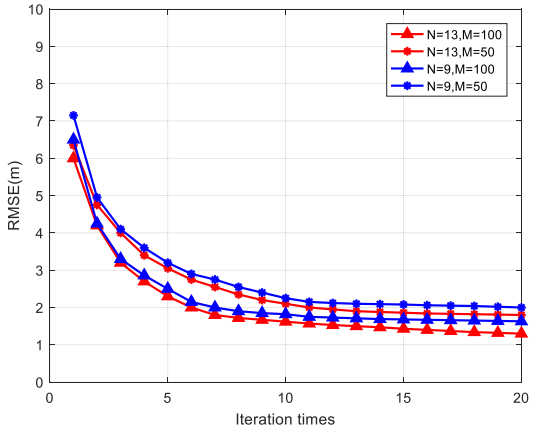

FIGURE 8. The influence of the number of undetermined nodes and the number of anchor nodes on the positioning performance in the network(RMSE).

C. THE INFLUENCE OF THE NUMBER OF UNDETERMINED NODES AND THE NUMBER OF ANCHOR NODES

The impact of the number of undetermined nodes and the number of anchor nodes on the positioning performance was analyzed in Figure 8 and 9 respectively. The simulation parameters were: Number of anchor nodes M= 13/9, number of undetermined nodes N= 100/50. The information ambiguity of node prior location was 10m, standard deviation of ranging error was 1m, and the Monte Carlo simulation time was $T = 500$ times.

It can be seen from Figures 8 and 9 that when the number of anchor nodes was 13 and the number of undetermined nodes was 100, the positioning performance was the best, and the positioning accuracy of 90% nodes was 2m. When the number of anchor nodes was constant, the positioning accuracy increased as the number of undetermined nodes increased. This was because the more undetermined nodes involved, the cooperative neighbor information received by each node increased, then improved the positioning performance of underwater nodes.

When the number of undetermined nodes in the network was kept constant; the more the number of anchor nodes, the better the positioning performance was. More anchor nodes meant more neighbor nodes with high reliability location information provided by the undetermined

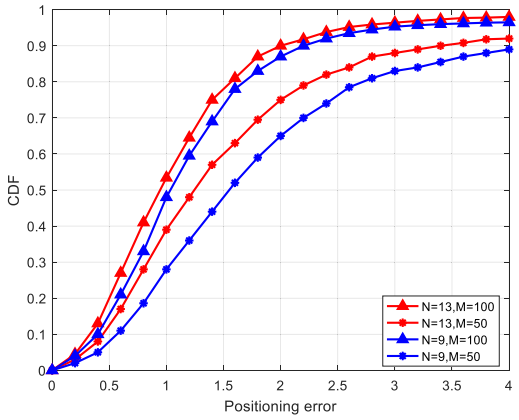

FIGURE 9. The influence of the number of undetermined nodes and the number of anchor nodes on the positioning performance in the network(CDF).

nodes, and the improved positioning performance of underwater nodes.

D. COMPARISON OF DIFFERENT POSITION ALGORITHMS

The positioning performance of the GPI-CP algorithm proposed in this paper was compared with the SPAWN algorithm which proposed by prof. Van [13] and the Taylor-VMP algorithm which proposed by prof. Cakmak [17]. The comparison results are shown in Figures 10 and 11 respectively. The simulation was set as: number of anchor nodes M= 13, undetermined nodes N= 100. The information ambiguity of node prior location was 10m, standard deviation of ranging error was 1m. The number of particle samples of SPAWN algorithm was 500, time of Monte Carlo simulation was T= 500 times.

It can be seen from Figure 10 that the positioning errors of the three algorithms decreased with the increase of iteration time and gradually tended to converge. Spawn algorithm had the best performance and the highest convergence speed, because it adopted a large number of weighted particles to express messages. The more the particles, the higher the positioning accuracy was. The GPI-CP algorithm proposed in this paper adopted the way of parameter information expression and transmission, and its positioning performance was very close to that of SPAWN algorithm. When the algorithm converges completely, the RMSE of our proposed algorithm is the smallest. Compared with the SPAWN algorithm, the position performance is improved by 10%, and compared with the Taylor VMP algorithm, the position performance is improved by 30%.

The comparison results of computational complexity and communication calculation between the GPI-CP algorithm, SPAWN algorithm and Taylor-VMP algorithm are shown in Table 2. K represents the number of particles and N_i represents the number of neighbor undetermined nodes. The computational complexity of the SPAWN algorithm was significantly larger. It was directly proportional to the product of the number of neighbor nodes Ni and the square of

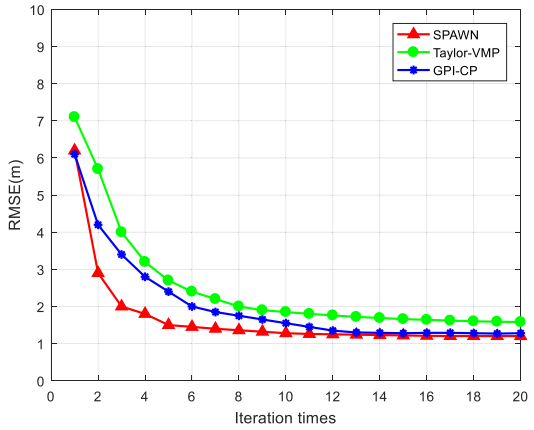

FIGURE 10. Positioning performance comparison between GPI-CP algorithm and SPAWN algorithm(RMSE).

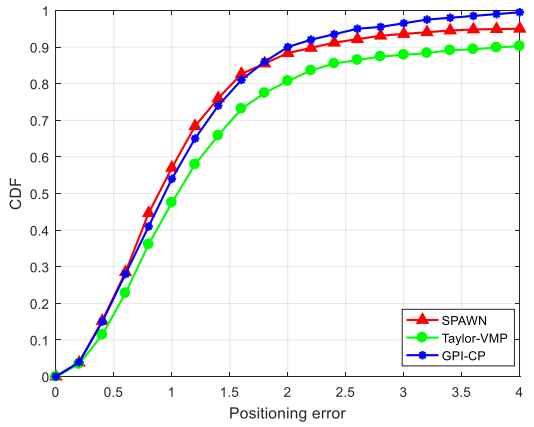

FIGURE 11. Positioning performance comparison between GPI-CP algorithm and SPAWN algorithm (CDF).

particle number k of the undetermined nodes, while the GPI-CP algorithm and Taylor-VMP algorithm were only related to N_i. As for the Communication calculation, both the GPI-CP algorithm and Taylor-VMP algorithm adopted Gaussian approximation. Each underwater node only needed to transfer four Gaussian parameters (x-axis mean and variance, Y-axis mean and variance) per time. However, each node of the SPAWN algorithm needed to transfer k particles and k weight coefficients each time, so the communication calculation was very large. Therefore, in specific and practical applications, a compromise between positioning performance, computational complexity and communication calculation can be considered in order to choose a positioning algorithm with better comprehensive performance.

E. TEST EXPERIMENT IN POOL ENVIRONMENT

In the laboratory pool test, the pool in Chang'an campus of Northwest Polytechnic University was adopted for the experiment. The size of cooperative node position was 100m * 100m, and the ranging and communication calculation between each underwater node was equal. The underwater node modules independently developed by the research group were adopted. The positioning results

TABLE 2. Comparison of computation complexity and communication calculation between GPI-CP algorithm and SPAWN algorithm.

Algorithm	Computational complexity	Communication calculation
SPAWN	$O(K^2 N_i)$	K particles and Kweight coefficients
GPI-CP	$O(N_i)$	4parameters
Taylor-VMP	$O(N_i)$	4parameters

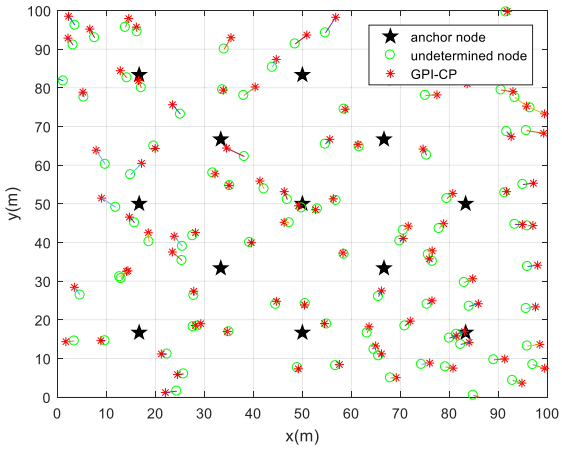

FIGURE 12. Single test positioning performance of GPI-CP algorithm.

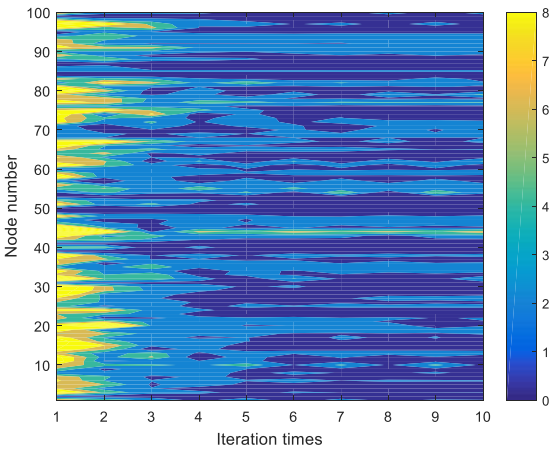

FIGURE 13. Positioning deviation contour map of 100 undetermined nodes.

of the algorithm are shown in Figure 12. The positioning error contour map of all undetermined nodes after multiple iterations is shown in Figure 13. The simulation was set as: the number of anchor nodes M= 13, and the number of undetermined nodes N= 100. The standard deviation of ranging error between nodes was set as 1m, standard deviation of location ambiguity was 10m.

In Figure 13, the blue line connecting the real position and the estimated position of the undetermined nodes represents the positioning error. As can be seen from Figure 12, except for the undetermined nodes at the right boundary coordinates

(100,83), other underwater nodes had high positioning accuracy, which is because the number of cooperative neighbor nodes (including anchor nodes and cooperative nodes) of the boundary point was small, resulting in large deviation in position estimation. Figure 13 shows the contour map of positioning error of 100 undetermined nodes after 20 iterations. It can be seen from Figure 13 that after 20 iterations, the positioning accuracy of most underwater nodes is less than 1.6m, and that the positioning accuracy of node 3 to be located is about 19m, which corresponds to the boundary underwater nodes with large positioning deviation as shown in Figure 12.

VI. CONCLUSION

In view of the high complexity and low efficiency of the existing underwater cooperative position algorithms, the first-order Taylor expansion algorithm was adopted at the estimation location of the undetermined nodes and the neighbor nodes. The Gaussian parameterization of all messages was combined with the factor graph theory and the product principle to realize the underwater distributed cooperative position. The simulation analyzed the proposed algorithms from three aspects: ambiguity setting, ranging deviation and the number of nodes. In the aspect of location ambiguity, the convergence of all nodes could be completed by about eight iterations, and the fluctuation deviation of overall location ambiguity could be reduced by more than 80%. In terms of ranging error, the convergence of the whole cooperative position nodes could be completed by about ten iterations, and the ranging error could be reduced by more than 10%. In terms of the number of nodes, the more the underwater nodes, the better the performance gain, and the smaller the increment of computational complexity. The simulation comparison was conducted with the existing algorithms in the comprehensive environment, and the results proved that the algorithm proposed by this paper has lower computational complexity and better cooperative position performance, as well as a better prospect for application in the underwater distributed cooperative position network system. In the future work, we will combine the BP-based method with the covariance intersection technique to minimize the uncertainty in correlations and achieve fast computing in the network of intelligent unmanned underwater vehicle.

ACKNOWLEDGMENT

The authors would like to thank editors for rigorous work and the anonymous reviewers for their comments and suggestions.

REFERENCES

[1] J. Shao, D. Luo, Y. Xu, and H. Duan, "Cooperative path planning for multiple robots with motion constraints in obstacle-strewn environment," *IEEE Access*, vol. 7, pp. 132286–132301, 2019.
[2] L. Zhang, C. Tang, Y. Zhang, and H. Song, "Inertial-navigation-aided single-satellite highly dynamic positioning algorithm," *Sensors*, vol. 19, no. 19, p. 4196, 2019.
[3] C. Tang, L. Zhang, Y. Zhang, and H. Song, "Factor graph-assisted distributed cooperative positioning algorithm in the GNSS system," *Sensors*, vol. 18, no. 11, p. 3748, 2018.
[4] C. Tang, L. Zhang, Y. Zhang, and H. Song, "Bidirectional satellite communication under same frequency transmission with non-linear self-interference reduction algorithm," *IET Commun.*, vol. 12, no. 1, pp. 52–58, Jan. 2018.
[5] C. Tang, L. Zhang, Y. Zhang, and Z. Yue, "Nonlinear revised error aided feedback equalization in high-speed satellite communication," *Telecommun. Syst.*, vol. 66, no. 2, pp. 243–251, Oct. 2017.
[6] X. Chen, W. Gao, and J. Wang, "Robust all-source positioning of UAVs based on belief propagation," *EURASIP J. Adv. Signal Process.*, vol. 2013, no. 1, p. 150, Dec. 2013.
[7] J. Fernandez-Bes, L. A. Azpicueta-Ruiz, J. Arenas-García, and M. T. M. Silva, "Distributed estimation in diffusion networks using affine least-squares combiners," *Digit. Signal Process.*, vol. 36, pp. 1–14, Jan. 2015.
[8] Z. G. Jun, L. Xin, X. Z. Long, and L. H. Chao, "Weighted least square localization algorithm based on RSSI values," in *Proc. 5th Int. Conf. Instrum. Meas., Comput., Commun., Control*, 2015, pp. 1236–1239.
[9] M. Leng, W. P. Tay, and T. Q. S. Quek, "Cooperative and distributed localization for wireless sensor networks in multipath environments," in *Proc. Int. Conf. Acoustics, Speech Signal Process. (ICASSP)*, 2012, pp. 3125–3128.
[10] R. M. Buehrer, H. Wymeersch, and R. M. Vaghefi, "Collaborative sensor network localization: Algorithms and practical issues," *Proc. IEEE*, vol. 106, no. 6, pp. 1089–1114, Jun. 2018.
[11] A. F. Garcia-Fernandez, L. Svensson, and S. Sarkka, "Cooperative localization using posterior linearization belief propagation," *IEEE Trans. Veh. Technol.*, vol. 67, no. 1, pp. 832–836, Jan. 2018.
[12] P.-A. Oikonomou-Filandras and K.-K. Wong, "HEVA: Cooperative localization using a combined non-parametric belief propagation and variational message passing approach," *J. Commun. Netw.*, vol. 18, no. 3, pp. 397–410, Jun. 2016.
[13] T. V. Nguyen, Y. Jeong, H. Shin, and M. Z. Win, "Least square cooperative localization," *IEEE Trans. Veh. Technol.*, vol. 64, no. 4, pp. 1318–1330, Apr. 2015.
[14] R. M. Vaghefi and R. M. Buehrer, "Cooperative localization in NLOS environments using semidefinite programming," *IEEE Commun. Lett.*, vol. 19, no. 8, pp. 1382–1385, Aug. 2015.
[15] R. M. Abdelmoneem and E. Shaaban, "Locally centralized SOCP-based localization technique for wireless sensor network," *Procedia Comput. Sci.*, vol. 73, pp. 76–85, Jan. 2015.
[16] H. Wymeersch, J. Lien, and M. Z. Win, "Cooperative localization in wireless network," *Proc. IEEE*, vol. 97, no. 2, pp. 427–450, Feb. 2009.
[17] B. Cakmak, D. N. Urup, F. Meyer, T. Pedersen, B. H. Fleury, and F. Hlawatsch, "Cooperative localization for mobile networks: A distributed belief propagation-mean field message passing algorithm," *IEEE Signal Process. Lett.*, vol. 23, no. 6, pp. 828–832, Jun. 2016.
[18] H. Kim, S. W. Choi, and S. Kim, "Connectivity information-aided belief propagation for cooperative localization," *IEEE Wireless Commun. Lett.*, vol. 7, no. 6, pp. 1010–1013, Dec. 2018.
[19] B. Chen and D. Pompili, "Modeling position uncertainty of networked autonomous underwater vehicles," *Ad Hoc Netw.*, vol. 34, pp. 184–195, Nov. 2015.
[20] M. Jouhari, K. Ibrahimi, H. Tembine, and J. Ben-Othman, "Underwater wireless sensor networks: A survey on enabling technologies, localization protocols, and Internet of underwater things," *IEEE Access*, vol. 7, pp. 96879–96899, 2019.
[21] Y. Cong, X. Zhou, B. Zhou, and V. K. N. Lau, "Cooperative localization in mobile wireless networks with asynchronous measurements and communications," *IEEE Access*, vol. 7, pp. 125442–125462, 2019.

LINGLING ZHANG (Member, IEEE) received the Ph.D. degree in communication and information engineering from Northwestern Polytechnical University, Xi'an, Shannxi, China, in May 2016. She is currently an Associate Professor with the Northwestern Polytechnical University. She is also a Visiting Scholar with the University of Virginia. She is the author of more than 20 articles. She is a coauthor of two books and over ten patent families. Her research interests include underwater communication and underwater cooperative position.

CHENGKAI TANG (Member, IEEE) received the Ph.D. degree in communication and information engineering from Northwestern Polytechnical University, Xi'an, Shannxi, China, in May 2015. He is currently an Associate Professor with Northwestern Polytechnical University. He is also a Visiting Scholar with the University of Virginia. He is the author of more than 30 articles. He builds the State Key Laboratory for intelligent navigation. He is a coauthor of four books and over ten patent families. His research interests include intelligent position, underwater communication, and cooperative navigation.

PEILIN CHEN received the master's degree in communication and information engineering from Northwestern Polytechnical University, Xi'an, Shannxi, China, in March 2011. He is currently a Senior Engineer with The 54th Research Institute of China Electronics Technology Group Corporation, Shijiazhuang, China. He is the author of more than ten articles. His research interests include satellite navigation, MIMO communication, and cooperative navigation.

YI ZHANG received the B.S. degree from Xidian University, Xi'an, Shannxi, China, in 1983, and the M.S. degree in control engineering and the Ph.D. degree in communication and information engineering from Northwestern Polytechnical University, Xi'an, in 1995 and May 2010, respectively. She is currently a Professor with Northwestern Polytechnical University. She is the author of more than 200 articles. She is a coauthor of 20 books and over 50 patent families. Her research interests include cooperative communication and cooperative navigation.